The Effect of Beam Depth on the Seismic Behavior of Flange Plate Connections Between Steel Beam and Box

A. Deylami, **M. Tehranizadeh** & **M. Gholami**
Amirkabir University of Technology, Iran

15 WCEE
LISBOA 2012

SUMMURY

This paper presents analytical and experimental studies on the cyclic behavior of flange plate connection between a steel beam and a welded box column. Two full-scale specimens were tested to evaluate the effect of beam depth on the seismic response of flange plate connection. The flange plate connection in the test specimens achieved the AISC seismic provision requirements for special moment frames. The test results indicate that a deeper beam can lead to a greater potential for fracture in the groove weld joining the beam web to the beam flange at the plastic hinge region. Then, the finite-element model developed using ABAQUS was validated using the test results. The validated finite element model was subsequently used to further investigate the behavior of the test specimens.

keywords: Connections; Flange Plate; Box Columns; Steel beam; Experimental program; Finite element analysis; beam depth

1. INTRODUCTION

Box columns are frequently employed in areas of high seismic risk because they have an excellent capacity to resist biaxial bending. Cold-formed hollow sections are often used for low and medium rise buildings and built-up sections made up of four plates welded together are used for high rise buildings (Nakashima et al, 2000). Extensive studies have been carried out and several new connection details have been proposed for the connection of I-beams to wide flange columns since the 1994 Northridge earthquake (Kim et al, 2002, Ricles et al, 2002, Chen et al, 2005, Tabar et al, 2004, Shiravand et al, 2010, Adeli et al, 2011). But limited research for the connection of I-beams to box–columns has been conducted (Chen et al, 2004). Kim et al. (2004) tested two full-scale moment connections to US box columns fabricated using pre-Northridge connection details. Test results revealed that both specimens failed by brittle fracture of complete joint penetration (CJP) welds between the beam flange and the column during a story drift angle of less than 1% rad, which resulted in no plastic rotation in the connections. Chen et al (2004) tested six large scale specimens of steel beam-to-box column connections. One of the test specimens was the unreinforced connection using pre-Northridge details, and other test specimens were the reinforced connections using rib plates or wing plates. The unreinforced connection was failed by fracture in the heat affected zone (HAZ) of the beam bottom flange during 2.3% story drift angel cycle.

In the present study the behavior of a moment resisting connection, shown in Fig. 1, has been investigated. This type of connection is mainly fabricated on site. The geometry of these plates is considered in a manner that site welding in a horizontal position is possible for connecting flange plates to beam and column.
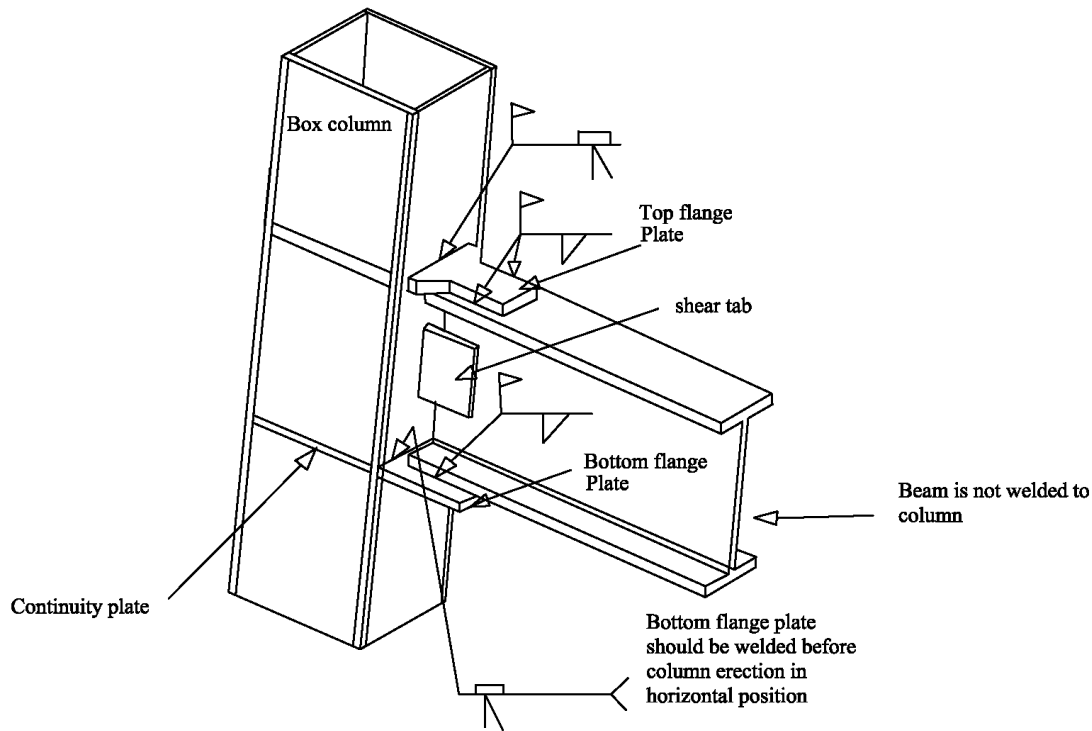
Figure 1. Field welded moment connection.

In this study, two full-scale specimens with welded flange plate connection were tested to evaluate the effect of beam depth on the seismic response of flange plate connections. The results of the specimen's hysteretic behavior were obtained and compared to the AISC seismic provision requirements in order to qualify the flange plate connections.

2. EXPRIMENTAL PROGRAM

The behavior of the moment connections under severe cyclic loading, particularly in regard to the initiation and propagation of fracture, cannot be reliably predicted by analytical means alone. Consequently, the satisfactory performance of connections must be confirmed by laboratory testing. Therefore, an experiment was carried out to clarify the seismic behavior of the flange plate connections. The testing procedure and test results for global and local seismic behavior of the test specimens are presented in the following sections.

2.1. Test specimens

Two large-scale specimens were designed to simulate an exterior T-shaped joint subassembly. Each subassembly contained a column between the mid-height of the two adjacent floors and a half-span of the beam. The general configuration of the subassembly is shown in Fig. 2. To consider the practical aspects, the size of the beam and the column sections in specimens was selected from exterior connections of a 20 stories building. The building was designed according to AISC 360-05 and AISC 341-05 provisions.

Summary information on the specimens is presented in Table 2.1. Fig. 3 shows connection details of specimen BD53. Beam geometry of specimen BD53 was identical to that of BD33 except that the beam depth was increased from 330 to 530 mm. Note that a doubler plate was added to the panel zone of specimen BD53 to ensure that all specimens have approximately the same panel zone strength to beam strength ratio. This is especially important since panel zone rotation can affect on the response

of connections. The panel zone and beam strengths are calculated according to the AISC seismic provision.
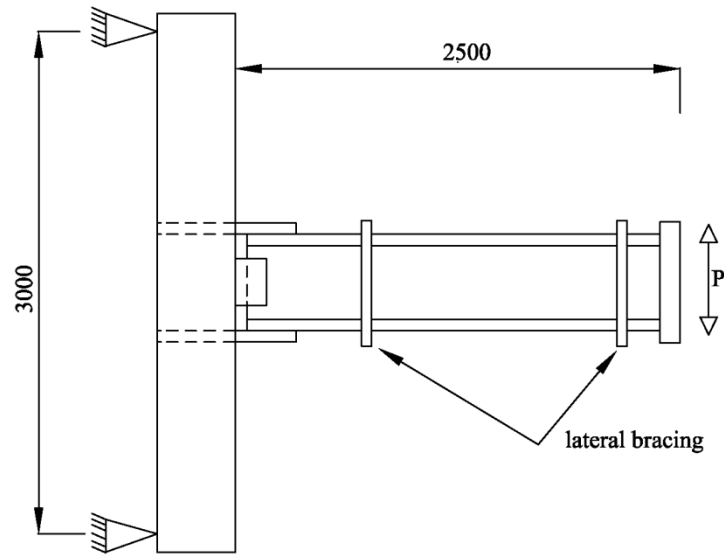

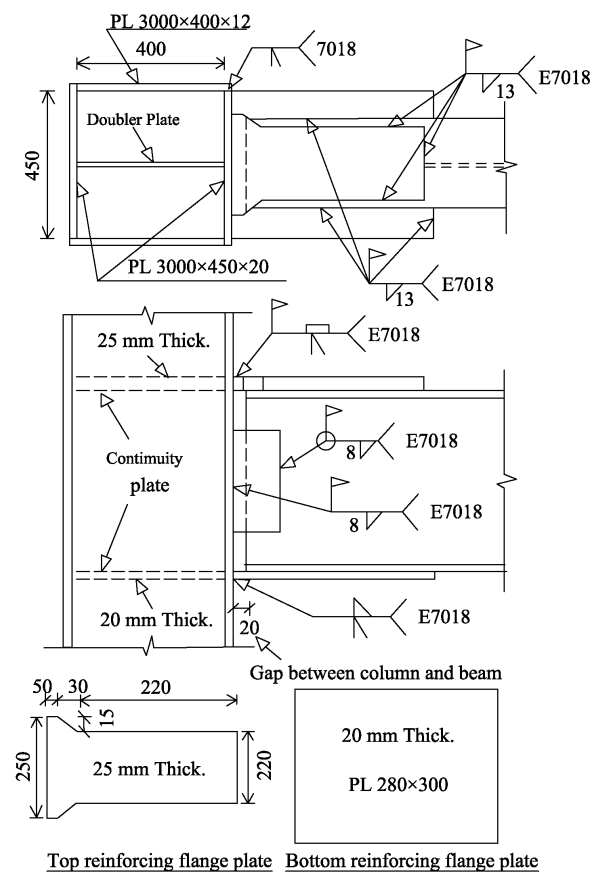**Figure 2.** Configuration of the exterior joint subassembly

Figure 3. Connection details of specimen BD53

Table 2.1. Summary Information on specimens

specimen	Beam size	Column size	Beam length	doubler plate	Panel zone strength to beam strength ratio
BD53	H-530×250×10×15	B-450 × 400 × 20 × 12	2500	15	1.1
BD33	H-330×250×10×15	B-350 × 400 × 20 × 20	2500	--------	1.1

Note: All dimensions in mm.

2.2. Test setup and instrumentation

According to the shape of the specimens, a test setup was prepared to simulate the boundary conditions of the exterior joint subassembly in a laterally loaded moment frame. The column top and bottom were supported by real hinges. The beam was laterally braced in the vicinity of the plastic hinge and also near the beam end. The general configuration of the test setup is shown in Fig. 4. The cyclic displacement proposed by AISC seismic provisions was applied at the tip of the beam by a hydraulic actuator.

Figure 4. Test setup configuration

2.3. Test observations

Figs. 5 and 6 show the test specimens BD33 and BD53 at the end of the test, respectively. In the both test specimens, plastic hinge forms in the beam at the nose of flange plates. Such a result is desirable

because the objective of the flange-plate connection is to force inelastic action in the beam away from the column face.

In the specimen BD53, tearing was occurred in the groove weld joining the beam web to the beam flange at the plastic hinge region, as shown in Fig. 6. In contrast, no crack was observed in the specimen BD33. This result indicates that a deeper beam can lead to a greater potential for fracture in the groove weld joining the beam web to the beam flange at the plastic hinge region. There is a possible explanation for this result:

A deeper beam results in a higher plastic strain in the groove weld joining the beam web to the beam flange at the plastic hinge region due to an increase in the amplitude of beam flange local buckling. The higher plastic strain increases potential for fracture .
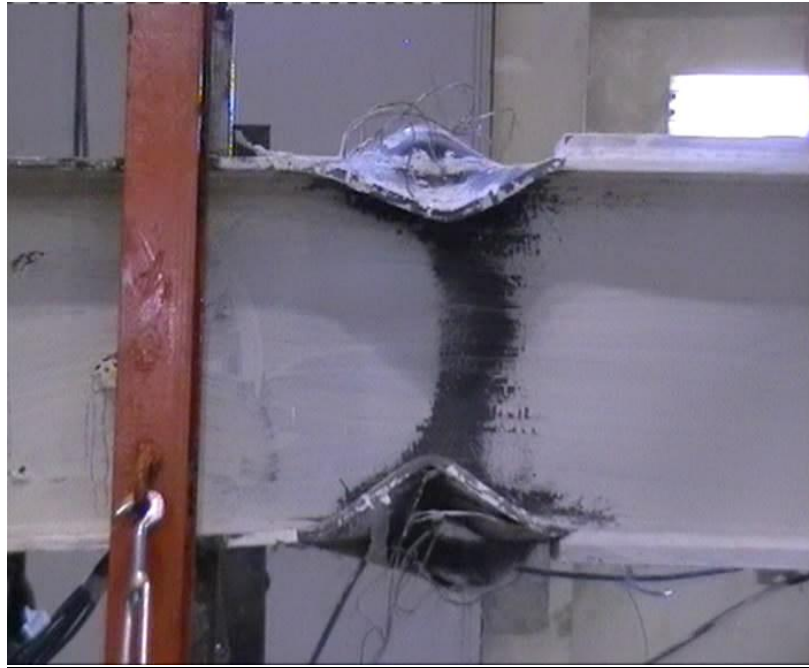

**Figure 5.** Specimen BD33 at the end of the test.

**Figure 6.** Fracture at the groove weld joining the beam web to the beam flange in the BD53

2.4. General evaluation of the connection behavior

The hysteretic curves of the moment at the column face versus story drift angle (θ) for test specimens BD33 and BD53 are presented in Fig. 7. The story drift angle is computed by dividing the total beam tip displacement by the distance from the beam tip to the column centerline. In the test specimens, moment resistance at 4% total story drift was more than 80% plastic moment of beam. Therefore, flange plate connection in the specimens achieved the AISC seismic provision requirements for special moment frames. It should be noted that the strength degradation of the specimens resulted from beam flange and web buckling during the cyclic loading.

In specimen BD53, the peak moment resistance is reached at 2% rad story drift, followed by a fairly rapid deterioration in strength with increasing drift due to flange and web local buckling. In contrast, peak resistance in specimens BD33 is reached at 4% rad and the rate of post peak connection strength degradation is markedly slower. The rate of strength degradation of the moment resistance in connections is related to the amplitude of beam flange local buckling. For connection with deeper beam, buckling amplitudes are larger and the rate of strength degradation is higher.
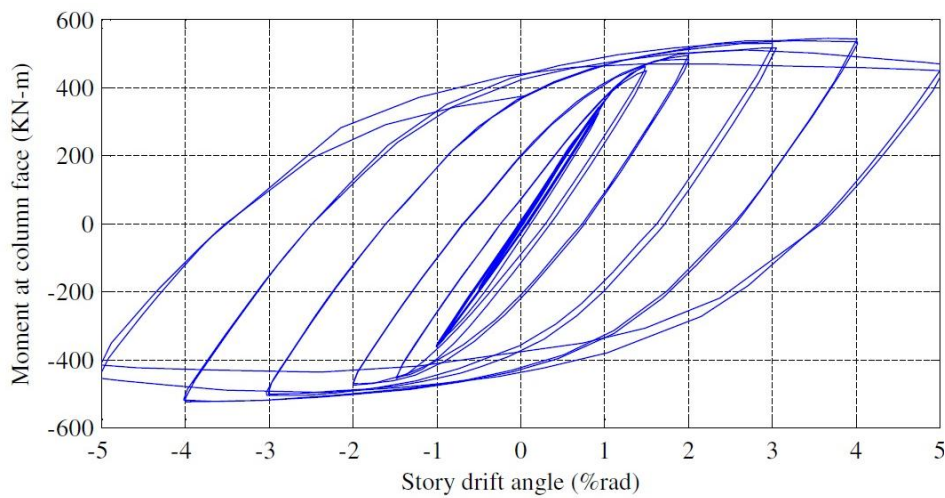
a)
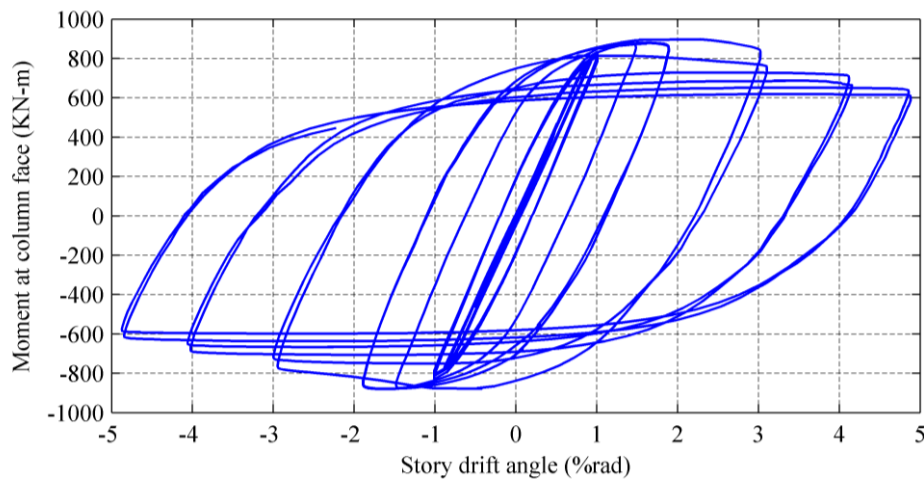
b)

Figure 7. The hysteretic curves for test specimens a) BD33 and b) BD53

3. NONLINEAR FINITE ELEMENT ANALYSIS

Finite-element analysis can provide considerable insight into behavior of test specimens.

3.1. Finite element modeling

ABAQUS models of BD53 and BD33 were prepared. As shown in Fig. 8, groove welds and fillet welds were modeled. The beam, column, plates, CJP groove welds and fillet welds in the model were discretized using three-dimensional solid (brick) elements. The size of the finite-element mesh varied over the length and height of the model. A fine- mesh was used near the connection of the beam to the column and the beam flange to the reinforcing plate. A coarser mesh was used elsewhere. Most of the solid elements were right-angle prisms. Hinged boundary conditions were used to support the column top and bottom. The load was applied by imposing incremental vertical displacements at the beam tip during the analysis.

Data from tests of coupons extracted from the beam and column of specimen were used to establish the stress-strain relationships for the beam and column elements. The weld material was modeled using the test data of Kaufmann (1976). Table 3.1 presents the material properties used for the analytical models. A bilinear stress-strain relationship was assumed for each of the components identified in Table 3.1. The Poisson's ratio was taken as 0.3 for all materials throughout the analyses. To account for material nonlinearities, the von mises yield criterion was employed.
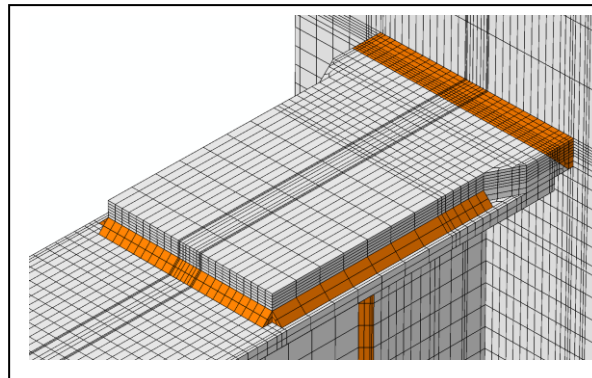

Figure 8. Finite element model

Table 3.1. Material properties used for the analytical models

	Yield point		Ultimate point	
Component	Stress (Mpa) σ_y	Strain (%) ε_y	Stress (Mpa) σ_u	Strain (%) ε_u
Beam flange	3050	0.15	4200	18
Beam web	2900	0.145	4100	18
Column flange	2700	0.135	3650	15
Column web	2700	0.125	3650	14
Reinforcing plates	2650	0.1225	3600	15
Continuity plates	2650	0.1275	3700	15
Weld material	5250	0.26	5600	12

3.2. Model validation

The finite element analysis of models BD53 and BD33 were performed. The cyclic outcomes are compared with the cyclic experimental results. As shown in Fig. 9 the experimental and finite element results of BD53 are in good agreement. While the ultimate load and initial stiffness are well evaluated, the extant differences between the two data sets are justified by geometric differences

between the finite element models and specimens, uncertainties in the material model, and also unavoidable residual stresses.
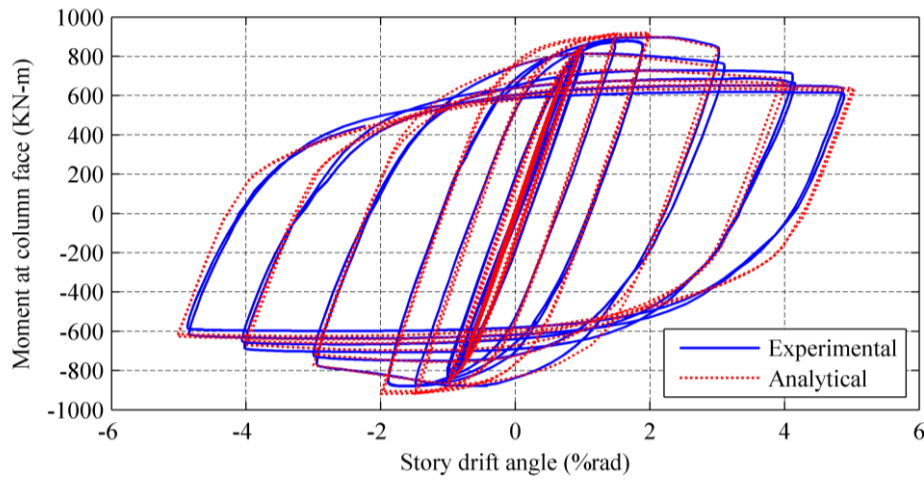

b)

**Figure 9.** Combined plot of experimental and analytical results for specimen BD53

3.3. PEEQ distribution in the specimens

The validated models were used to evaluate the PEEQ distribution in the test specimens. Fig. 10 presents the PEEQ contours in the finite element models BD53 and BD33. The key observations from Fig. 10 are 1) finite element models exhibited behavior as observed in the test specimens in the way of forming plastic hinge in the beam at the nose of flange plates, 2) The maximum PEEQ value of BD53 is substantially larger than that of BD33. This result indicates that a deeper beam results in a higher plastic strain at the plastic hinge region.

Fig. 11 presents the PEEQ contours in the groove weld joining the beam web to the beam flange at the plastic hinge region for models BD53 and BD33. The maximum PEEQ value of BD53 is substantially larger than that of BD33. For this reason, the tearing was occurred in the groove weld at the plastic hinge region of specimen BD53 (as shown in Fig. 6).
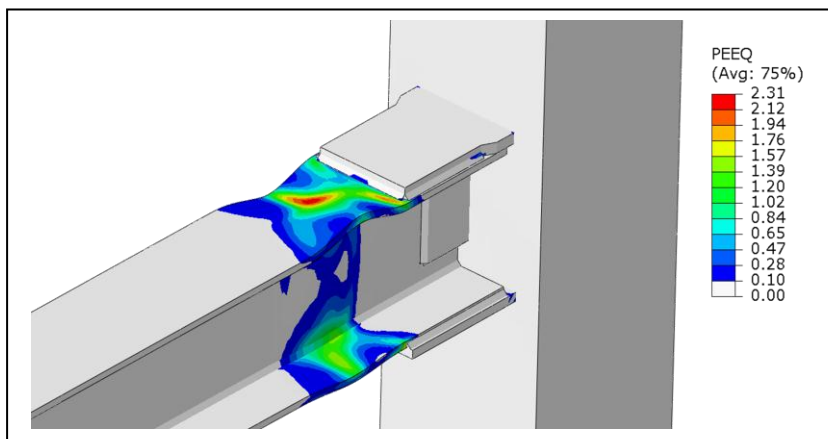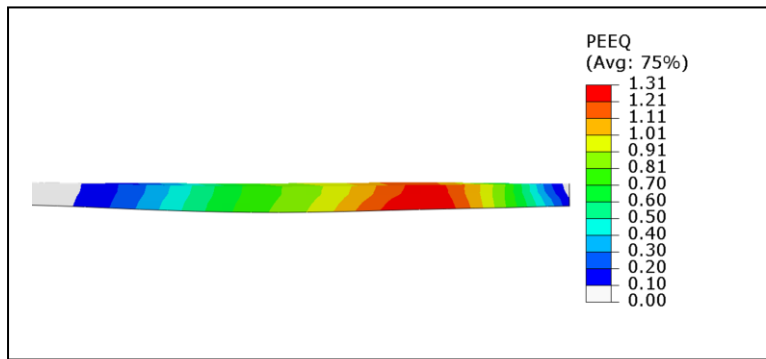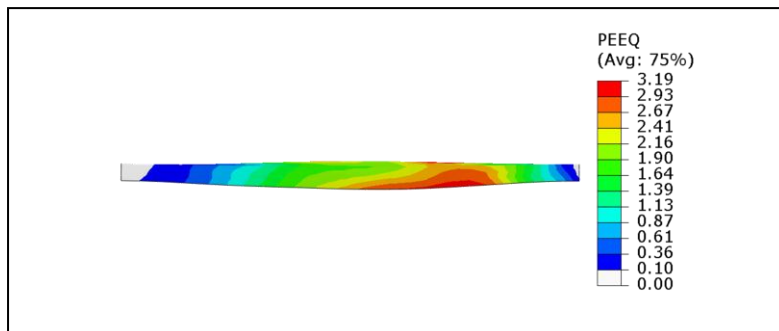

a)
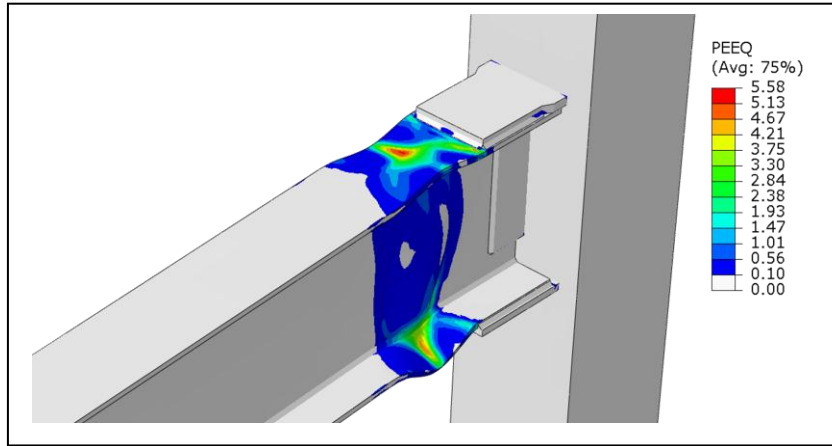
b)

Figure 10. Equivalent plastic strain distribution in the finite element models a) BD33, b) BD53

a)

b)

Figure. 11. Equivalent plastic strain distribution in the groove weld joining the beam web to the beam flange at the plastic hinge region for models a) BD33, b) BD53

4. CONCLUSIONS

Two full-scale specimens with flange plate connections were tested to evaluate the effect of beam depth on the seismic response of connection. Flange plate connection in the test specimens achieved the AISC seismic provision requirements for special moment frames. Then, a validated finite element

model was used to further investigate local response in the test specimens. The key conclusions drawn from the analytical studies and the associated experimental results are:

1. A deeper beam can lead to a greater potential for fracture in the groove weld joining the beam web to the beam flange at the plastic hinge region.

2. For connection with deeper beam, buckling amplitudes are larger and the rate of strength degradation is higher.

REFERENCES

Nakashima, M., Roeder, CW. and Maruoka, Y. (2000). Steel moment frames for earthquakes in United States and Japan. *J Struct Eng* **126:8**, 861–8.

Kim T., Whittaker AS., Gilani ASJ., Bertero VV. and Takhirov SM. (2002). Cover-plate and flange-plate steel moment-resisting connections. *Journal of Structural Engineering* **128:4**, 474–482.

Ricles JM., Fisher JW., Lu LW. and Kaufmann EJ. (2002). Development of improved welded moment connections for earthquake-resistant design. *Journal of Constructional Steel Research* **58:4**, 565–604.

Chen CC., Chen SW., Chung MD. and Lin MC. (2005). Cyclic behavior of unreinforced and rib-reinforced moment connections. *Journal of Constructional Steel Research* **61:6**, 1–21.

Tabar, A.M. and Deylami, A. (2004). Investigation of major parameters affecting instability of steel beams with RBS moment connections. *Steel and Composite Structures* **6:3**, 1475-1491.

Shiravand, M. and Deylami, A. (2010). Application of Full Depth Side Plate to Moment Connection of I-Beam to Double-I Column. *Advances in Structural Engineering* **13:6**, 1047-1062.

Adeli, M., Banazadeh, M. and Deylami, A. (2011). Bayesian approach for determination of drift hazard curves for generic steel moment-resisting frames in territory of Tehran. *International Journal of Civil Engineering* **9: 3**, 145-154.

Chen CC., Lin CC. and Tsai CL. (2004). Evaluation of reinforced connections between steel beams and box columns. *Engineering Structures* **13:5**, 1089–1092.

Kim T, Whittaker AS, Gilani ASJ, Bertero VV, Takhirov SM, Ostertag C, 2002 ", Forensic studies of a large cover plat steel moment resisting connection" The Structural Design of Tall Buildings 11, 265–283.

Kaufmann, E. J. (1997). Dynamic tension tests of simulated moment resisting frame weld joints.Chicago. Steel Tips, Structural Steel Education Council, *American Institute of Steel Construction* .